Georgia Journal of Science

Volume 81 *No. 2 Scholarly Contributions from the Membership and Others* Article 15

2023

Perovskite CsPbBr3 Solar Cells With Novel Hole-Transporting Layer of Metal Complexes

Liqiu Zheng
Albany state university, liqiu.zheng@asurams.edu

Evynn S. Jackson
Albany State University, ejacks35@students.asurams.edu

Ny'kesha S. Warren
Albany State University, nwarren3@students.asurams.edu

Robert Owor
Albany state university, robert.owor@asurams.edu

Zhongrui Li
University of Michigan, zhongrui@umich.edu

Perovskite CsPbBr3 Solar Cells With Novel Hole-Transporting Layer of Metal Complexes

Acknowledgements

Acknowledgements: This work was supported by National Science Foundation (NSF) (Grant No. 1700339).

Perovskite $CsPbBr_3$ Solar Cells with Novel Hole-Transporting Layer of Metal Complexes

Liqiu Zheng,[1]*Evynn S Jackson,[1] Ny'kesha S Warren,[1] Robert Owor,[1] and Zhongrui Li [2]
[1]Natural Sciences Department, Albany State University, 504 college ave, Albany, GA31705, USA
[2]Electron Microbeam Analysis Laboratory, University of Michigan, Ann Arbor MI 48109, USA
*Corresponding Author: *Liqiu.Zheng@asurams.edu*

ABSTRACT

For the first time, the novel application of Schiff-base copper complexes in all-inorganic perovskite $CsBrBr_3$ solar cells has been explored and turns out they could be utilized as effective hole-transporting materials. Schiff-base copper complexes with halogen ligands (R=Cl and Br) are synthesized with an ease approach at a low cost, both of which exhibit decent power conversion efficiency of 4.55% and 5.71%, respectively, when being constructed into solar devices as hole transport layers. Thanks to high thermal/chemical stability of those Schiff-base metal complexes, the strengthened stability was achieved which is comparable to that of carbon-based $CsBrBr_3$ solar cells. Although the power conversion efficiency is not as competitive as expected, the great potential exists for further optimizing the functionality of perovskite solar devices by finely tuning the photovoltaic properties of those Schiff-base metal complexes through coordinating ligands or replacing with other transition metals.

Keywords: Built-in potential; Heterojunction; Hole transporting layer; Perovskite solar cells; Power conversion efficiency.

INTRODUCTION

The solid thin film perovskite solar cells (PSCs), most likely in the form of a planar n-i-p (or inverted p-i-n, even p-n) heterojunction, have been intensively examined and employed because of the simple device configuration and outstanding device efficiency, which have even outperformed the prevalent silicon-based solar cells, as indicated in "NREL efficiency chart". In the planar structure, the "n" refers to an electron transporting material (ETM), usually adopting semiconductors like TiO_2 or ZnO for collecting electron carriers. The "i" is an intrinsic light absorbing layer of perovskite materials. The instability in the ambient conditions of the inorganic-organic hybrid perovskites like $CH_3NH_3PbX_3$ ($MAPbX_3$) or $HC(NH_2)$ BbX_3($FAPbX_3$)

(in which X=Cl, Br or I), necessitates the substitution of the organic part MA or FA for an inorganic portion, for instance, cesium, in spite of the better photovoltaic conversion efficiency (PCE) of hybrid perovskites. While "p" stands for a hole transporting material (HTM) in the device which essentially collects hole carriers and blocks electrons to follow through. Although a variety of materials have been attempted for hole transporting layers from organic options like poly(2,4,6-trimethyl-N,N-di-ptolylaniline (PTAA) or 2,20 ,7,70 -tetrakis [N,N-di-(4-methoxyphenyl)amino]-9,90 -spirobifluorene (spiro-OMeTAD) to inorganic materials like copper thiocyanate (CuSCN) or Cu_2O and CuO as reported by Sharmoukh et al. (2020), the HTM in the most efficient organic–inorganic or inorganic-based PSCs with the conventional structure (n–i–p) is still spiro-OMeTAD, as reported by Wang et al.(2019). Regardless of its better performance, it has become increasingly apparent that the incumbent spiro-OMeTAD is not an ideal choice for HTM due to the high cost of production, even at volume, and instability upon exposure to oxygen, moisture, UV-radiation and temperature. In practice, the required additives for increased performance of spiro-OMeTAD and related HTMs come at a cost to stability. More importantly, the spiro core in spiro-OMeTAD poses a daunting complicated synthetic challenge which requires several sequential steps including a Grignard reaction, a cyclization reaction, a bromination reaction and a Hartwig–Buchwald coupling, with total yield less than 40% in the report of Ma et al. (2020). It is high time to identify better candidate materials with high stability, low cost, and simplified synthetic processing for the PSCs because as an equally critical component, the HTM exerts a tremendous impact on the PCE and stability of the solar devices.

Due to their widespread applications in various areas including nonlinear optics, molecular/metal ion sensing, dye-sensitized solar cells, molecular magnetism and photoluminescence as in Tian et al. (1997),Lin et al. (2021), Kagatikar et al. (2021), Zheng et al.(2020), and Aazam et al.(2012). Schiff-base and their complexes with transition metals have attracted tremendous attention in numerous fields thanks to their exceptional properties as shown in Kitamori et al.(2019) and Kato et al.(2020), such as, intense absorption in the visible region, high conductivity, ambipolar transporting properties, excellent photophysical and electronic properties, thermal/chemical stability and etc. An azomethine group (–N=C–) containing Schiff-base could be produced through the condensation reaction between the carbonyl groups and primary amines as in Hugo et al.1864. Salen ligands fall into the category of Schiff-base. Salen ligands can form complexes with virtually all metals, affording an advantage

to finely tune optical and electrochemical properties through adding electron-withdrawing or electron-donating substituents on the salen framework or changing the metal center of the complexes. Consequently, the highest occupied molecular orbital-lowest unoccupied molecular orbital (HOMO-LUMO) energy gap is conveniently regulated through the interaction of the d-orbitals of the transition metal with the HOMO and/or LUMO of the ligand. Meanwhile, based on the coordination number, geometry and valence shell of the selected metal atom, high diversity of the molecular framework is achieved. Moreover, as an excellent alternative to porphyrins, the tetradentate binding site of salen-ligands is similar to the porphyrin framework. However, salen complexes are more easily synthesized with considerably lower cost compared with porphyrins.

Among the Schiff-base metal complexes, Cu complexes have resurfaced lately in inorganic synthesis investigations with rapt attention as they have been successfully applied for low-cost and highly efficient solid-state dye-sensitized solar cells due to their better carrier mobility as reported by Sharmoukh et al. (2020) and Wang et al. (2020). Inspired by the idea, for the first time, Schiff-base Cu complexes with R=Cl and Br will be adopted as HTM and constructed into solar devices with perovskite $CsPbBr_3$ (all-inorganic perovskite with relative high stability) in this work, in hopes of achieving better functionality of the PSCs with a structure of FTO/TiO_2/$CsPbBr_3$/Schiff-base copper complexes/Al, which is as same as the configuration of FTO/TiO_2/$CsPbBr_3$/carbon/Al with the record high stability as in Chang et al.(2016).

MATERIALS & METHODS

The synthesis of regular-sized all-inorganic $CsPbBr_3$ adopts a facile one–step solution process, as reported by Li et al. (2017). Schiff-base copper complexes are synthesized with an ease approach at a lower cost. An ethanol solution of 3,5-dichlorosalicylaldehyde (2 mmol, 0.382 g in 25 ml ethanol) or 3,5-dibromosalicylaldehyde (2 mmol, 25 ml) is put into an ethanol solution of 3, 4-diaminobenzoic acid (1 mmol, 25 ml). The mixture is stirred and refluxed at 70 °C–80 °C for 4–6 h to yield an ethanol solution of ligands. An aqueous solution of 1mmol (0.20 g) of Copper (II) acetate monohydrate is then added, and the solution is refluxed for 4 hours at 70 °C–80 °C, and the precipitate is filtered from the ice-cooled mixture and washed with 50% ethanol, followed by drying under a vacuum to afford Schiff-base Cu complexes reported by Zheng et al. (2020). The steps for construction of the solar cells were detailed in the previous

report by Zheng et al. (2021). Instead of utilizing carbon, Schiff-base copper complexes in ethanol solutions are ultrasonicated and then the homogenous solutions are spin-coated into thin films as HTM for the solar cells.

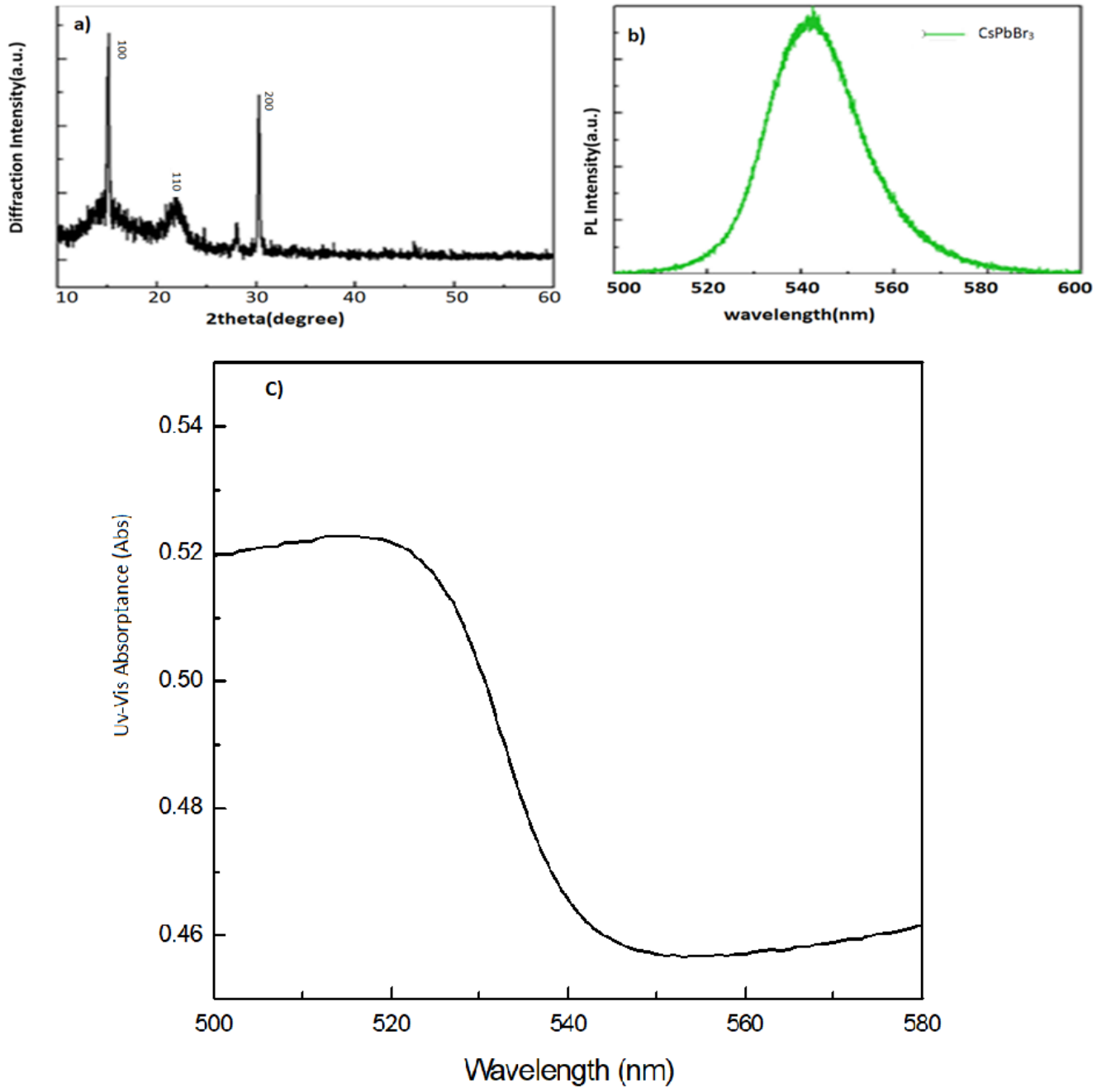

Figure 1.a) X-ray Diffraction Pattern for $CsPbBr_3$ b) Photoluminescence Spectroscopy C) Uv-Vis absorptance of CsPbBr3

The UV-vis optical absorption spectra were recorded in a transmission mode on a Varian Cary Bio 50 UV-Visible Spectrophotometer. Fourier-transform infrared spectra (FTIR) were collected by using a Thermo Scientific™ Nicolet™ iS50 FTIR spectrometer, as an all-in-one materials analysis workstation which features purpose-built accessories and integrated software. X-ray diffraction (XRD) data was acquired on a Rigaku Ultima IV diffractometer with copper *K*-alpha line (λ = 154.059 pm) as the light source. The current density–voltage characteristic curves of the devices were evaluated both in the dark and under an AM1.5 illumination (100 mW cm^{-2}) by a Keithley 2400 source meter. The photovoltaic performance of devices was measured from an area of 1× 1 cm^2 under a small-area class-B solar simulator (PV Measurements, Inc.).

RESULTS AND DISCUSSION

$CsPbBr_3$ is obtained as a yellowish polycrystalline powder. As revealed by the XRD profile in Figure 1a), $CsPbBr_3$ is pure and presents the characteristic distortion defined in the orthorhombic symmetry, space group (62) *Pbnm* with lattice constants *a*=8.1843 Å, *b*=8.2334 Å and *c*=11.7268 Å, as reported by López et al. (2020). Figure 1b) displays the photoluminescence (PL) spectrum. The $CsPbBr_3$ sample with emission band peaks at 540 nm, which shows exciton absorption bands roughly at 530 nm in the Ultraviolet-visible (UV-vis) absorption, as shown in figure 1c) and is consistent with the report of Li et al. (2020). The sample has a Stokes shift of 10 nm. The PL band is considered to result from the emission of excitons explained by Chen et al. (2019) in which strong interactions between electrons and phonons produce small polarons that tend to bind charge carriers and result in trapped/bound excitons. The successful synthesis of pure crystal $CsPbBr_3$ will act as the intrinsic light absorbing material in $CsPbBr_3$-based solar devices.

The crystal structure and chemical composition of the synthesized complexes are scrutinized by XRD as shown in Figure 2. The XRD measurements are performed at 2θ = 10–80° revealing that both complexes are crystalline in nature and the crystal structures of both are very similar. Figure 3 clearly exhibits that Schiff-base copper complexes with R=Cl possess diffraction peaks around 2θ = 15.5°, 19.5°, 20.6°, 24.5°, 25.3°, 27.1°, and 34.7°, with the R=Br peaks slightly down shifted to lower angles with respect to those of R=Cl, indicating the R=Br complexes have a bit large lattice constant. The powder patterns are indexed by Monte Carlo and grid search as

implemented in the program McMaille by Bail et al. (2004). The indexing results show triclinic crystalline structure. For the R=Cl complex, *a*=7.81Å, *b*=6.99 Å, *c*=9.31 Å, α=107.8°, β=67.8°, γ=

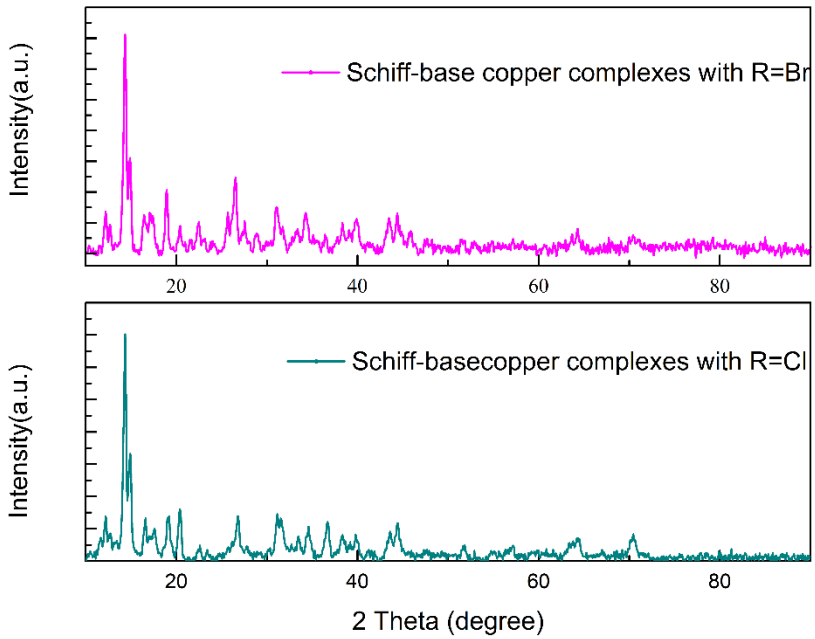

Figure 2. X-Ray Diffraction patterns for Schiff-base copper complexes with R=Br(top) and R=Cl(bottom)

93.8°, while the R=Br complex has the lattice constants *a*=10.68 Å, *b*=8.87 Å, *c*=7.83 Å, α=108.2°, β=101.6°, γ=92.7°. The 2-theta peak positions and the intensities can be extracted from a peak hunting program based upon a pseudo powder pattern. The results are consistent with the previous studies of Zheng et al. (2020) and Ejidike et al. (2018). The crystallite size of Schiff-base Cu complexes can be estimated from the full width at half maximum of diffraction peaks by following Debye–Scherrer equation, expressed as the formula: $t=K*\lambda/(\beta*\cos\theta)$, in which *t* is the calculated grain size of the sample, λ is the wavelength of X-ray source (about 0.154 nm in this case), β is the broadening measured as the full width at half maximum (FWHM) in radians, θ is the Bragg diffraction angle and *K* is a correction constant (typically~0.9). The crystal sizes of both Schiff-base copper complexes are close, and both are in nano-meters, varying from 24.51 nm to 65.85 nm.

Figure 3 demonstrates the ultra-violet visible absorption spectra of obtained Schiff-base copper (II) complexes (R=Cl and R=Br), in which both display very close absorbing behaviors except for slightly stronger absorbance of the R=Br complex. The similar characteristic absorbance bands of both complexes appear at 470 nm which suggest the square planar geometry around Cu (II)

centre since the observed λ_{max} values are used to predict the geometry around the central metal ion in the complex as indicated by Lacroix et al. (1996). The characteristic bands for both at 470 nm are attributed to $^2B_{1g} \rightarrow {}^2A_{1g}$ transition, indicating Cl or Br does not noticeably influence electronic band structures of both complexes. At the same time, the spectra of ligands show

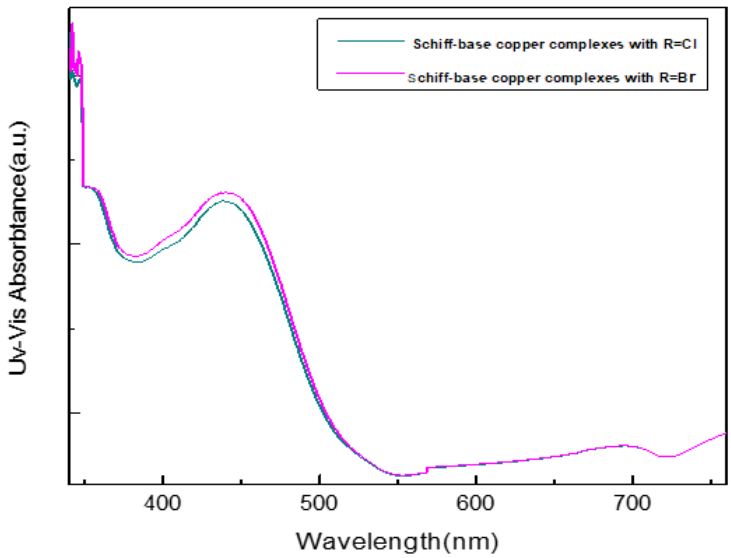

Figure 3. Ultra-violet visible absorption for Schiff-base copper (II) complexes

similar absorption bands at 290 nm, which verify the presence of n→n* and π→π* transitions of their azomethines chromophore group and aromatic ring. The charge transfer transition due to metal to ligand π-back bonding may also contribute to these absorption bands (below 400 nm) in the complexes, consistent with the results of Antony et al. 2012. λ_{max} for ligand and its copper (II) complexes are below 400 nm and 470 nm, respectively, confirming the complex formation. There are very weak broad bands also appearing between 723- 757 nm in the spectra for both complexes, ascribed to d–d transitions ($^2E_g \rightarrow {}^2T_{2g}$) for Cu (II) complexes resulting from a tetragonal distortion geometry due to the Jahn–Teller effect, reported by Hazra et al. (2014). This d-d transition can be enhanced with a very high-concentration solution of the complexes. It suggests the presence of additional levels around -3.35 to -3.5 eV coming from the d-like SOMO levels. These orbitals are δ-like for the ligands, and the oxidation occurs on the HOMO rather than the SOMO. It is expected from the HOMO levels that these complexes display hole conductivity by Deivanayagam et al. (2014) and Koyama et al. (2020). As natural p-type conductivity, Schiff-base Cu(II) complexes have been attempted to dope into spiro-OMeTAD for enhanced carrier mobility and long carrier diffusion length. Meanwhile, solar cells with spiro-

OMeTAD with dopants of Schiff-base Cu (II) complexes as HTM stayed stable for 20 days, reported by Chen et al. (2017). What's more, the conductance values of 54, 62 and 66 Ω^{1} cm^{2} correspond to cobalt (II), nickel (II) and copper (II) complexes respectively, suggesting Schiff-base copper complexes possessing the highest conductivity among those complexes, interpreted by Joseyphus et al. (2012).

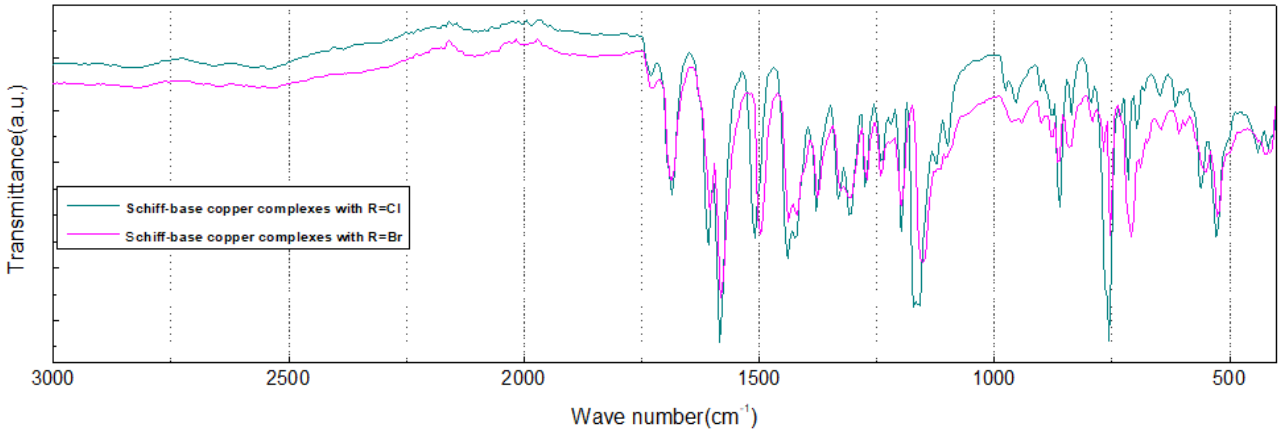

Figure 4. Fourier transform infrared Spectra of Schiff-base Copper Complexes

Fourier transform infrared spectroscopy (FTIR) is a fast, easy, and reliable technique for identifying materials and quantification of constituents. Figure 4 reveals very similar patterns of both complexes except that the overall peaks of R=Cl complexes shift to the higher wavenumber because of the reduced mass as the frequency of vibration is inversely proportional to mass of vibrating molecule. The sharp oscillations at 1684 cm^{-1} (in R=Cl complexes) and 1688cm^{-1} (in R=Br complexes) evidence the presence of carbonyl groups (C=O) of acid. The peaks at 1609.93cm^{-1} (in R=Cl Complexes) and 1606 cm^{-1} (in R=Br complexes) corroborate the presence of C=N groups in both complexes, which is supposed to be at 1624 cm^{-1}. Expectedly, the coordination of nitrogen center to the metal ion could reduce the electron density in the azomethines link and shift the C=N Stretching frequency to the lower wave number. This lower shift might be inherent from a weakening in the C=N bond after complexation based on the donation of an electron from the imine nitrogen to the copper ion empty d-orbital, Yusuf et al. (2021). The shift in C=N stretch in the complexes verifies the successful coordination of azomethines nitrogen to the metal (copper) center. The peaks obtained at 1583 cm^{-1}(in R=Cl Complexes) and 1580 cm^{-1} (in R=Br complexes) are associated with aromatic C=C groups. The

peaks (in R=Cl Complexes) obtained at 1274.53 cm^{-1} and 1308.07 cm^{-1} account for C-C group and C-O group, while in R=Br complexes, they are at 1270 cm^{-1} and 1304 cm^{-1}, respectively. The peaks observed at 715.52 cm^{-1} and 756.52 cm^{-1} substantiate the presence of C-Cl groups, while in R=Br complexes, the peaks of C-Br group appear at 708.07 cm^{-1} and 752.79 cm^{-1}. The peaks around 439.75cm^{-1} (in R=Cl complexes) and 421.84cm^{-1} (in R=Br complexes) suggest the presence of Cu-N bands; The peaks at 529 cm^{-1} (in R=Cl complexes) and 525 cm^{-1}(in R=Br complexes) are assigned to Cu-O bands. These ν(Cu–N) and ν(Cu–O) stretching bonds indicate the imine (C=N) and phenoxide (O–) groups coordinated with Cu (II) ions. The coordination facilitates the formation of chelated complexes confirmed by the single-crystal structure of the complexes, as reported by Lacroix et al.1996 and Jenisha et al. (2015).

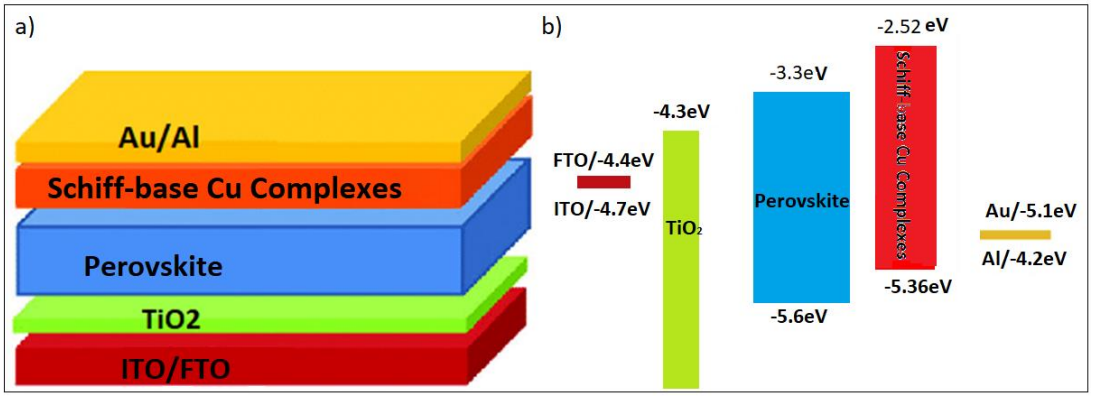

Figure 5. a) schematic diagram of n-i-p planar structure of PSC, and (b) schematic energy level diagram of the constituent materials in the PSC.

Photovoltaic performance is evaluated by the PCE of the solar devices. In spite of the success in solid state dye-sensitized solar cells, to our best knowledge Schiff-base copper complexes have never been utilized as HTM in $CsPbBr_3$ based solar cells. For the first time, Schiff-base copper complexes are attempted as HTM in perovskite solar cells with a structure as diagrammed in Figure 5a). In the devices, aluminum is adopted as metal electrodes which have the high work function with enhanced optical properties at a lower cost. The energy levels of each component are well aligned as sketched in Figure 5b) by referring to experimental and theoretical results calculated by density functional theory of Yusuf et al. 2021, Li et al. (2019) and Silva et al. (2022). Evidently, the HOMO energy levels of those complexes are more over that of the perovskite

conduction band (-3.30 eV), which indicates that the hole carriers could be energetically favorable to “bubble up”, being collected by the complexes.

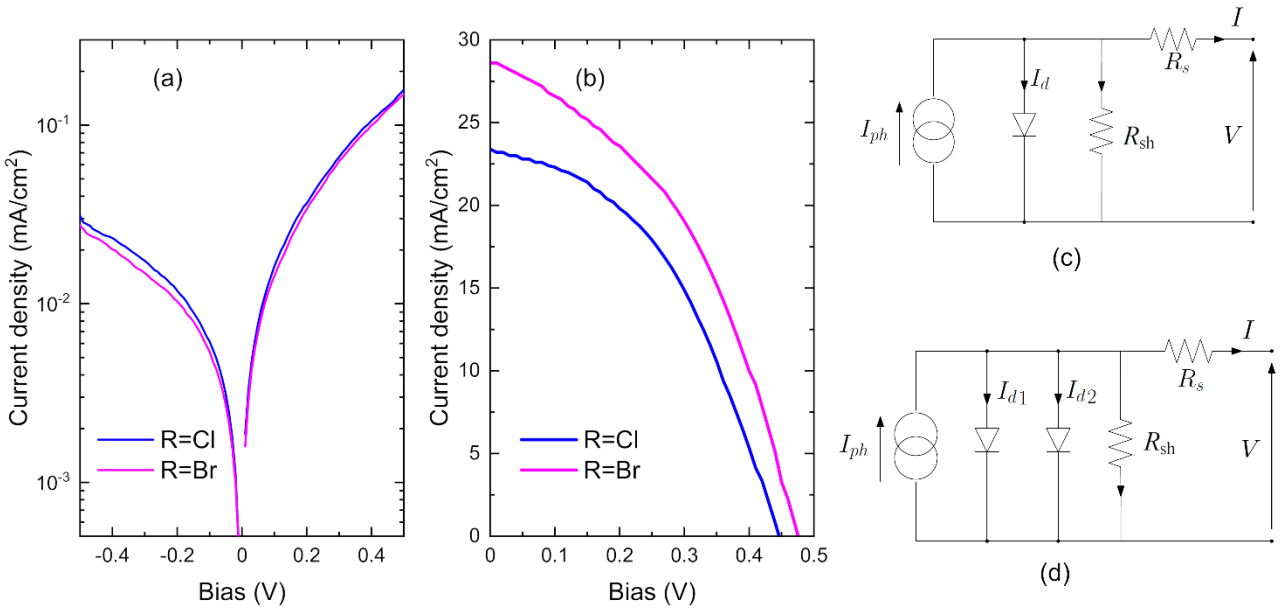

Figure 6. Photovoltaic performance evaluated by a) dark and illuminated currents of J-V curves for both cells b) illuminated current flipped into first quadrant for efficiency calculation. (c) single and(d) double diode equivalent circuit models of a solar cell

The dark currents of both Cl- and Br-devices show rectifying characteristic behaviors of a diode as shown in Figure 6(a). Figure 6(b) shows that under the identical conditions, the PCE of Cl-devices with 4.55% is comparable to that of Br- solar cells with 5.71%. Being slightly lower is due to the relatively higher electron affinity of the Schiff-base Cu complexes with R=Cl than that of ones with R=Br. The higher electron affinity of the Schiff-base copper complexes with R=Cl affects the hole transporting capability, which is detrimental in the PCE. To extract the solar cell parameters from the illuminated IV curves, both a single-diode and a double-diode models are adopted in the full pattern fitting via particle-swam-optimization approach (PSO), as reported by Kennedy et al. (1995), Shi et al. (1998), and Ebrahimi et al. (2019). For the single-diode model, the current delivered by the cells under illumination can be expressed as in terms of the photocurrent J_{ph}, the current J_d through the diode and the leakage current Js according to the following relationship:

$$J = J_L - J_d - J_{sh} = J_L - J_s\{exp[\frac{q(V+JR_s)}{nkT}] - 1\} - \frac{V+JR_s}{R_{shunt}}, \quad (1)$$

where J_s is the reverse saturation current of the diffusion phenomenon, n is the quality factor of the diode, which is between 1 and 2, Rs is series resistance, R_{sh} is shunt resistance, T the temperature of operating cell, k is the Boltzmann constant, and q is the charge of an electron. The double-diode equivalent circuit of a solar cell is a current source in parallel with two diodes considering which represent the diffusion and the recombination phenomena, as explained by Hovinen et al. (1994), respectively, and two resistances which are the shunt resistance and series resistance. The I-V characteristic of the double-diode model is expressed by the following equation:

$$J = J_{ph} - J_{d1} - J_{d2} - J_{sh} = J_L - J_{01}\{exp[\frac{q(V+JR_S)}{kT}] - 1\} - J_{02}\{exp[\frac{q(V+JR_S)}{2kT}] - 1\} - \frac{V+JR_S}{R_{shunt}}, \quad (2)$$

where the "ideality factors" in the denominators of the argument of the exponential term are set as of n_1=1 and of n_2=2, respectively for the first and second diodes, to represent the diffusion (J_{o1}) and recombination current (J_{o2}) terms. The internal parameters of the two devices are extracted by the PSO approach and listed in Table 1. The photocurrent, series and shunt resistance are very comparable for both single-diode and double-diode models, confirming the reliability of the PSO fitting.

Based upon all listed parameters and compared the Cl- and Br- solar devices, the better light absorption of Schiff-base cu complexes with R=Br accounts for the photocurrent J_{ph} =28 mA/cm^2 of Br-devices, being slightly higher than that of Cl-solar cells with 23 mA/cm^2. Due to the similar band structures, the open circuit voltages are very close, with Voc=0.446 V for the Cl-cells and Voc=0.475 V for Br-devices, in which the difference might be caused by the slightly larger bandgap of R=Br metal complexes, which could not be clearly discerned by UV-vis absorption. Another cause is the relatively larger Rsh in Cl-cells which reduces the open circuit voltage. The relatively large Rs in Cl-cells decreases the short circuit current such that Jsc of 23.4 mA/cm^2 in Cl-cells is slightly lower than that (Jsc= 28.6 mA/cm^2) in Br-devices. A smaller recombination current in Br-cells counteracts it's a large diffusion current Js, which explains the slightly better PCE but still very close to that of the Cl-cells. As revealed by the UV-Vis spectra , an increase in the intensity is due to the d-d transition of the Schiff-base copper (II) complexes absorbing the light at wavelengths shorter than 550 nm, which also extended the electrode photo-response in the UV region, allowing the complexes to capture energy from both singlet and triplet excited states, elevating internal quantum efficiency's upper limit from 25% to nearly

100%, as shown in Zhang et al.(2019) and Camseil et al.(2007) which explains the relatively large current density in both samples. Therefore, the copper-based metal complexes can broaden the light-harvesting abilities and improve the efficiency by developing a new photoelectric conversion mechanism, ameliorating the charge injection and charge transporting when applied as charge transporting layers which consequently results in the relatively larger current density. In this configuration, not only does perovskite layer produce excitons, but also the metal complexes along with TiO_2 collectively produce excitons, which separate at interfaces due to built-in potentials contributing to the current density. The built-in potentials favor the exciton dissociation, which could enhance charge transfer from perovskite to ETL or HTL and reduce charge accumulation at the interface by facilitating charge separation and increasing recombination resistance. Moreover, Schiff metal complexes have been reported as effective sensitizers for perovskite for visible-light conversion with photovoltage of 0.97 V and power conversion efficiency about 3.8%, as reported by Wang et al. (2017). As visible light passes through the transparent electrode into perovskite layer, in which excite electrons flow into the conduction band of TiO_2. The electrons from TiO_2 then flow toward the transparent electrode where they are collected for powering a load, increasing the current density.

Notedly, in both cases, the relatively lower shunt resistances, leading to smaller fill-factors, are attributed to the large size (1cm ×1cm) of the devices, which is very challenging to reduce defects and stop leakage current, as a result, the PCE for both devices is not as desirable as expected. However, due to the high thermal/chemical stability, Khalaji et al. (2015) reported that the Schiff-base-copper complex solar cells demonstrate exceedingly strengthened stability, even being comparable to that of carbon-based $CsPbBr_3$ solar cells, which have the record-high stable operating time.

The significant practical role of hole transport materials played in solar cells has been highlighted in this work, although the photovoltaic performance of the PSCs hinges on multiple parameters of each constituent like improving the quality of each layer by reducing defects or optimizing the thickness of each layer and so on. As far as the HTM is concerned, further work on Schiff-base metal complexes is essential to regulate the photovoltaic properties through coordinating ligands or replacing with other transition metals, for instance, to alter the energy

levels of these materials, as explained by Asiri et al. (2020), reaching a better alignment with the perovskite absorber, thus optimizing the performance of solar devices.

Table I. The internal parameters of the devices based on Schiff-base copper complexes (R=Cl and R=Br) obtained through the particle-swam optimization approach using both a single-diode and a double-diode models.

item	unit	R=C1 single-diode	R=Cl double-diode	R=Br single diode	R=Br double-diode
J_{ph}	mA/cm²	23.45	23.45	28.83	28.74
J_s / J_{o1}	mA/cm²	3.61E-3	6.55E-9	2.21E-3	2.47E-7
J_{o2}	mA/cm²		4.03E-6		2.55E-6
n / n_1		1.976	1	1.968	1
n_2			2		2
R_s	Ohm/cm²	6.01	5.85	5.26	5.22
R_{sh}	Ohm/cm²	286.8	275.42	129.5	127.9
Voc	V	0.446	0.446	0.475	0.475
Jsc	mA/cm²	23.4	23.4	28.6	28.6
FF		0.44	0.44	0.42	0.42
efficiency	%	4.55	4.55	5.71	5.71

CONCLUSIONS

For the first time, the novel application of Schiff-base copper complexes in all-inorganic $CsBrBr_3$ has been explored and turns out they could be utilized as an effective hole transporting material with the comparable efficiency of 4.55% and 5.71%. Schiff-base copper complexes were synthesized with an ease approach at a low cost. The strengthened stability in ambient conditions, even being comparable with that of carbon-based $CsBrBr_3$ solar cells, is achieved thanks to high thermal/chemical stability of those complexes although the power conversion efficiency is not as desirable as expected, which still open the door for the great potential of this series of metal complexes in applications of the PSCs. Additional systematic investigation needs

to be done to finely tune the photovoltaic properties through coordinating ligands or replacing with other transition metals because changing the central metal can significantly ameliorate their photovoltaic properties like improving their light absorption, enhancing their carrier-transporting capabilities, or altering the energy levels of these materials, leading to a better alignment with the perovskite absorber, thus optimizing the solar device functionality.

Conflicts of interest

Authors declare there is no conflict of interest.

ORCID iDs

Liqiu Zheng https://orcid.org/0000-0002-9862-7105

REFERENCES

Aazam, E.S., A.F. EL Husseiny, and H.M. Al-Amria, 2012, Synthesis and photoluminescent properties of a Schiff- base ligand and its mononuclear Zn (II), Cd (II), Cu (II), Ni (II) and Pd (II) metal complexes, Arabian Journal of Chemistry, 5, 45-53.

Antony, D., R. Yadav, and R. Kalimuthu, 2012, Molecular and Biomolecular Spectroscopy, Spectrochimica Acta Part A11, 14-18.

Asiri, S., M. A. Kassem, M. A. Eltaher, and K. M. Saad, 2020, Novel Coordination Compounds Based on Copper Complexes with new Synthesized Schiff bases and Azo-dyes as Sensitizers for Dye-Sensitized Solar Cells: Spectral and Electrochemical Studies, International Journal of Electrochemical Science, 15 ,6508 – 6521, doi: 10.20964/2020.07.72.

Bail, A. Le, 2004, Powder Diffraction 19, 249-254.

Chang, X.W., W.P. Li, L.Q. Zhu, H.C. Liu, H.F. Geng, S.S. Xiang, J.M. Liu, and H.N. Chen, 2016, Carbon-Based CsPbBr3 Perovskite Solar Cells: All-Ambient Processes and High Thermal Stability, ACS Applied Material Interfaces, 8, 49, 33649–33655

Chen, C., W. Zhang, J.Y. Cong, M. Cheng, B.B. Zhang, H. Chen, P. Liu, R. F. Li, M. Safdari, L. Kloo, and L.C. Sun, 2017, Cu (II) Complexes as p-Type Dopants in Efficient Perovskite Solar Cells, ACS Energy Letter, 2, 497–503., DOI: 10.1021/acsenergylett.6b00691gy

Chen, H., A. Guo, J. Zhua, L. Cheng, and Q. Wang, 2019, Tunable photoluminescence of CsPbBr3 perovskite quantum dots for their physical research, Applied Surface Science, 465, 656-664.

Deivanayagam, P., R. Pa. Bhoopathy, and S. Thanikaikarasan, 2014, Synthesis, characterization, antimicrobial, analgesic and CNS studies of Schiff based Cu (II) complex derived from 4-choro-o-phenylene Diamine, International Journal of Advanced Chemistry,2, (2), 166-170.

Ebrahimi, S. M., E. Salahshour, M. Malekzadeh, and F. Gordillo, 2019, Parameters identification of PV solar cells and modules using flexible particle swarm optimization algorithm, Energy 179, 358-372.

Ejidike, I. P.,2018, Cu (II) Complexes of 4-[(1E)-N-{2-[(Z)-Benzylidene-amino] ethyl} Ethan imidoyl] benzene-1,3-diol Schiff Base: Synthesis, Spectroscopic, In-Vitro Antioxidant, Antifungal and Antibacterial Studies, Molecules, 29;23(7):1581. doi: 10.3390/molecules23071581.

Hazra, M., T. Dolai, A. Pandey, S. K. Dey, and A. Patra, 2014, Synthesis and Characterization of Copper (II) Complexes with Tridentate NNO Functionalized Ligand: Density Function Theory Study, DNA Binding Mechanism, Optical Properties, and Biological Application. Bioinorganic Chemistry and Applications, No. 104046.

Hovinen, A.,1994, Fitting of the Solar Cell /V-curve to the Two Diode Model, Physica Scripta 54, 175-176.

Jenisha, S., T. David, and J. P. Priyadharsini, 2015, Schiff base legand its complexes and their FTIR spectroscopy studies, International Journal on Applied Bioengineering, 9, 1-5.

Joseyphus, R. S., E. Viswanathan, C. J. Dhanaraj, and J. Joseph, 2012, Dielectric properties and conductivity studies of some tetradentate cobalt (II), nickel (II), and copper (II) Schiff base complexes, Journal of King Saud University - Science, 24, 233-236.

Kagatikar, S. and D. Sunil, 2021, Schiff Bases and Their Complexes in Organic Light Emitting Diode Application, Journal of Electronic Materials, 50, 6708–6723.

Kato, Y., K. Iijima, D. Yoo, T. Kawamoto, and T. Mori,2020, Ambipolar Transistor Properties of N 2 S 2 -Type Metal Complexes, Chemistry Letters, 49(7), DOI:10.1246/cl.200281.

Kennedy, J., and R. Eberhart, 1995, Particle Swarm Optimization, Proceedings of IEEE International Conference on Neural Networks. IV. 1942–1948. doi:10.1109/ICNN.1995.488968.

Khalaji, A. D. and D. Das, 2015, Thermal stability of copper (II) and nickel (II) Schiff base complexes, Journal of Thermal Analysis and Calorimetry, 120, 1529–1534.

Kitamori, T., D. Yoo, K. Iijima, T. Kawamoto, and T. Mori, 2019, Ambipolar Transistor Properties of Metal Complexes Derived from 1,2-Phenylenediamines, ACS Applied Electronic Materials, 1, 1633–1640, DOI: 10.1021/acsaelm.9b00344.

Koyama, K., K. Iijima, D. Yoo and T. Mori, 2020, Transistor properties of salen-type metal complexes, RSC Advances, 10, 29603.

Lacroix, P. G., S. D. Bella, and I. Ledoux,1996, Synthesis and Second-Order Nonlinear Optical Properties of New Copper (II), Nickel (II), and Zinc (II) Schiff-Base Complexes. Toward a Role of Inorganic Chromophores for Second Harmonic Generation, Chemistry of Materials, 8, 541-545.

Li, X., X.D. Mo, Y. Xiang, G.Z. Dai, P. He, M. Fang, J. Sun, H. Huang and J.L. Yang, 2020, High-performance and flexible CsPbBr3 UV–vis photodetectors fabricated via chemical vapor deposition, Journal Physics D: Applied Physics, 53, 354.

Li, X., Y. Tan, H. Lai, S.P. Li, Y. Chen, S.W. Li, P. Xu, and J.Y. Yang, 2019, All-Inorganic CsPbBr3 Perovskite Solar Cells with 10.45% Efficiency by Evaporation-Assisted Deposition and Setting Intermediate Energy Levels, ACS Applied Materials & Interfaces, 11 (33), 29746-29752.

Li, Y., Z.F. Shi, S. Li, L.Z. Lei, H.F. Ji, D. Wu, T.T. Xu, Y.T. Tian, and X.J. Li,2017, high performance perovskite photodetectors based on solution-processed all-inorganic CsPbX3 thin films, Journal of Materials Chemistry C, 5, 8355-8360. DOI: 0.1039/c7tc0213b.

Lin, L.Y., C. Lian, T. W. Jones, R. D. Bennett, B. Mihaylov, T.C-J Yang, J. T-W Wang, B. Chi, N. W. Duffy, J.H. Li, X.B. Wang, H. J. Snaith, and G. J. Wilson, 2021, Tunable transition metal complexes as hole transport materials for stable perovskite solar cells, Chemistry Communications, 57, 2093.

López, C. A., C. Abia, M.C. Alvarez-Galván, B. Hong, M. V. Martínez-Huerta, F. Serrano-Sánchez, F. Carrascoso, A. Castellanos-Gómez, M. T. Fernández-Dı´az, and J. A. Alonso, 2020, Crystal Structure Features of CsPbBr3 Perovskite Prepared by Mechanochemical Synthesis, ACS Omega, 5, 11, 5931–5938.

Ma, Z., Z. Xiao, Q.Y. Liu, D.J. Huang, W.Y. Zhou, H.F. Jiang, Z.Q. Yang, M. Zhang, W.F. Zhang, and Y.L. Huang, 2020, Oxidization-Free Spiro-OMeTAD Hole-Transporting Layer for Efficient CsPbI2Br Perovskite Solar Cells, ACS Applied Materials Interfaces, 12, 52779−52787.

Schiff, H., 1864, Mittheilungen aus dem Universitäts-laboratorium in Pisa: 2. Eine neue Reihe organischer Basen", Annalen der Chemie und Pharmacie (in German), 131: 118–119. doi:10.1002/jlac.18641310113.

Sharmoukh, W., S. A. AlKiey, B. A. Ali, L. Menon, and N. K. Allam, 2020, Recent progress in the development of hole-transport materials to boost the power conversion efficiency of perovskite solar cells, Sustainable Materials and Technologies, 26, e00210. https://doi.org/10.1016/j.susmat.2020.e00210.

Shi, Y., and R.C. Eberhart, 1998, A modified particle swarm optimizer, Proceedings of IEEE International Conference on Evolutionary Computation, 69–73. doi:10.1109/ICEC.1998.699146.

Silva, A. L.R., P.C.F.C. Oliveira, J. M. Gonçalves, V.M.F. Morais, and M.D.M.C.R. Silva,2022, Metal–ligand binding energies in copper (II) and nickel (II) complexes with tetradentate N2O2 Schiff base ligands, Inorganica Chimica Acta, 535, 24 ,120845.

Tian, Y.P., C.Y. Duan, X.Z. You, T. C. W. Mak, Q. Luo and J.Y. Zhou, 1997, Crystal structures, spectroscopic and nonlinear optical properties of metal complexes of Schiff-base ligands containing nitrogen and sulfur donors, Transition Metal Chemistry, 23, 17–20.

Wang, Y., X. M. Liu, T.Y. Zhang, X.T. Wang, M. Kan, J.L. Shi, and Y.X. Zhao, 2019, The Role of Dimethylammonium Iodide in CsPbI3 Perovskite Fabrication: Additive or Dopant? Angewandte Chemie (International ed.) 58, (46),16691-16696, https://doi.org/10.1002/anie.201910800.

Wang, Y.Z., W.K. Ye, X.B. Yang, E. Rezaee, H.Q. Shan, S. H. Yang, S. Y. Cai, J-H. Pan, J. J. Xu, and Z.-X Xu, 2020, Hole transport layers based on metal Schiff base complexes in perovskite solar cells, Synthetic Metals, 259, 116248.DOI: 10.1016/j.synthmet.2019.116248.

Yusuf, T. L., T. L. Yusuf, S. D. Oladipo, S. Zamisa, H. M. Kumalo, I. A. Lawal, M. M. Lawal, and N. Mabuba, 2021, Design of New Schiff-Base Copper (II) Complexes: Synthesis, Crystal Structures, DFT Study, and Binding Potency toward Cytochrome P450 3A4, ACS Omega, 6, 21, 13704−13718.

Zaumseil, J. and H. Sirringhaus, 2007, Electron and Ambipolar Transport in Organic Field-Effect Transistors, Chemical Reviews, 107, 1296-1323.

Zhang, J., L.L. Xu, and W.-Y. W, 2018, Energy materials based on metal Schiff base complexes, Coordination Chemistry Reviews, 355,180–198.

Zhang, W., P. Liu, A. Sadollahkhani, Y. Y. Li, B.B. Zhang, F.G. Zhang, M. Safdari, Y. Hao, Y. Hua, and L. Kloo ,2017, Investigation of Triphenylamine (TPA)-Based Metal Complexes and Their Application in Perovskite Solar Cells, ACS Omega, 2, 12, 9231−9240.

Zheng, L.Q., G. Page, and Z.R. Li, 2021, ZnO nanowire embedded TiO2 film as an electrode for perovskite CsPbI2Br solar cells, RSC Advances, 11, 19705, DOI: 10.1039/d1ra01563j.

Zheng, L.Q., T. H. Hurst, Z.R. Li, X.M. Zheng, C. C Nnyamah, and L. V. Wrensford, 2020, Salen Zn complexes along with ZnO nanowires for dye sensitized solar cells, Nano Express, 1, 010040.